Exploiting the Flexibility of District Heating System for Distribution System Operation: Set-Based Characterization and Temporal Decomposition

Weitao Chen, Xiaojun Wang, *Senior Member, IEEE*, Wei Wei, *Senior Member, IEEE*, Yin Xu, *Senior Member, IEEE*, Jianzhong Wu, *Fellow, IEEE*,

***Abstract*—The proliferation of distributed renewable resources increases the uncertainty in distribution systems. Coupling the distribution system and district heating system helps leverage the flexibility of thermal storage and thus supports the operation of the electrical grid. This paper proposes a method to characterize flexibility from district heating system via polyhedral sets. First, a recursive robust feasibility condition that ensures heat supply adequacy under uncertain demand is established. Then, stagewise robust feasible sets of thermal storage levels are calculated using a customized projection algorithm. Finally, dynamic bounds of electric heaters are computed by a further projection step. With those dynamic bounds, the electric heaters behave like reducible loads, and the demands in each period are decoupled over time, although the dispatch of thermal storage units must comply with inter-temporal constraints. The proposed method allows the two coupled systems to be operated in a distributed way without forecasts and extensive communications. Numerical simulations on small and practically sized testing systems validate the advantage of the proposed method. On average, the set calculation takes about 8 minutes for the day-ahead problem and 11 seconds for real-time dispatch on a portable laptop, and the prediction-free operation policy has an average optimality gap of 3.6% compared to the hindsight optimum.**

***Index Terms*—Distribution system, heating system, polyhedral projection, thermal energy storage, temporal decomposition.**

I. Introduction

With the increasing penetration of distributed renewable energy resources into the demand side, the uncertainty greatly challenges the operation of distribution network [1], where controllable units such as large thermal power plant is rare. Deploying battery storage is an option [2] to improve operation flexibility. However, the cost is still relatively high considering the lifetime of battery which is not very long.

In contrast, thermal energy storage (TES) is cheap and scalable. Meanwhile, electricity and heat are two main energy carriers on the demand side, but conventional boilers burn fossil fuels and produce considerable carbon emissions. Electrifying the heating system is beneficial to both critical infrastructures. The distribution system gains additional flexibility and reduces renewable power curtailment through making use of TES units in the heating system [3]; the heating system can reduce cost and carbon emission by using inexpensive and clean renewable energy at a lower contract price. Such a synergy makes electric boiler [4] and heat pump [5] increasingly popular, creating tight connections across the distribution system and the district heating system. Existing researches on the operation of coupled electricity and heating systems can be roughly categorized into four classes, depending on the cooperation mode and the way to cope with uncertainty.

The first class models both infrastructures in a centralized manner. It integrates the energy flow equations of two systems into a single deterministic problem. To investigate temperature distribution in a heating system, a nodal method is developed in [6]; it calculates the average temperature of all small water masses passing through a node in a given time interval. A hydraulic-thermal model for heating networks is proposed in [7], accounting for the water mass flow rates in pipelines. Combined heat and power dispatch of connected power and heating networks is studied in [8]. It proposes to leverage the thermal inertial of heating network as flexible demand and thus helps the power system better utilize wind power.

The second class considers uncertain renewable power and load demands in centralized dispatch. Robust optimization is a popular method as it requires little information regarding probability distributions. Robust scheduling of the integrated electricity and heating system is considered in [9], aiming to mitigate heating network uncertainties. An affinely adjustable robust method is set forth in [10] to dispatch multi-energy microgrids using piecewise linear decision rules. With the presence of TES unit and inter-temporal constraint, the anticipativity issue arises in some two-stage optimization methods. The operation of heating system must consider future demands because the thermal storage level is described by an inter-temporal constraint, and heat demands in future periods must be supplied to formulate the problem. As a result, the dispatch action in the current period is inevitably affect by uncertain parameters in the future, and hence may be suboptimal if the forecasts have nonnegligible errors. Non-anticipativity means that the dispatch action in the current period is independent of unknown parameters. The simplest non-anticipative policy is the greedy algorithm which can be myopic and also suboptimal. A good non-anticipative policy must be able to adaptively determine a tradeoff between the instant cost and future cost, which is a big challenge as exact forecast is not available.

This work was supported by the National Key Research and Development Program of China (2022YFB2405500). *(Corresponding Author: Yin Xu)*

W. Chen, X. Wang and Y. Xu are with the Department of Electrical Engineering, Beijing Jiaotong University, 100044 Beijing, China. (e-mail: chenweitao@bjtu.edu.cn; xjwang1@bjtu.edu.cn; xuyin@bjtu.edu.cn).

W. Wei is with the Department of Electrical Engineering, Tsinghua University, 100084 Beijing China (e-mail: wei-wei04@mails.tsinghua.edu.cn).

J. Wu is with the School of Engineering, Cardiff University, Cardiff CF24 3AA, U.K. (e-mail: wuj5@cardiff.ac.uk).

Non-anticipative methods for power system operation have been proposed. Affine policy is the most widely used one, such as that in [11]. It restricts the dispatch actions to be affine or piecewise affine functions in the uncertain parameters observed so far. Implicit policy [12] generates dynamic bounds that restrict the operating range of system facilities to ensure feasibility under uncertainty. A recent work in [13] reports an envelope-based policy optimization method for multistage robust dispatch of energy hubs, neglecting network constraints. A multistage robust optimization method is proposed in [14] for the integrated electric and heating system, ensuring the non-anticipativity of dispatch. By default, above works assume the system is managed by a dispatch center. This is true for industrial park level energy hubs, but may not be the case if the power and heating systems have larger sizes.

In general, city-sized distribution system and district heating system are operated by different entities. Neither of them has the data and models of the other system. With the deepened integration of two systems, coordinated operation can benefit both sides. To address this issue, the third class adopts a decentralized (horizontal) framework, aiming to develop distributed algorithms to help multiple agents which have similar size or volume on a spatial scale to make decisions without revealing private information. In [15], based on a marginal pricing-based market scheme, a decentralized operation is proposed for the interconnected power distribution network and district heating network. A dedicated optimization model is set forth in [16] to investigate the market impact of strategic providers and elastic demands. In [17], to protect private data of the electrical grid and the heating system, a decentralized algorithm based on Benders decomposition is proposed. In [18], an optimal power flow problem for the integrated electrical and heating systems optimization problem is solved alternatively by the consensus-based distributed algorithm. Ref. [19] establishes a transfer payment policy for heating and power systems, ensuring privacy, benefit, and mutual trust among each participant. In ref. [20], by considering the heating system with variable mass flow, a distributed dispatch method of integrated electricity-heat systems is proposed to improve operational flexibility. Robustness can be considered in decentralized method as well, such as those in [21] and [22]. Nonetheless, non-anticipativity of the dispatch policy remains an issue, and hyper parameters in the distributed algorithm must be well chosen to obtain good convergence performances.

The fourth class adopts a multi-layer (vertical) scheme, aiming to develop hierarchial algorithms by aggregating small distributed resources such as thermostatically controlled loads, distributed renewable resources, and batteries to reduce the complexity of analysis and computation. The work in [23] aggregates thermostatically controlled loads based on Minkowski sum method to provide a feasible operation set for the electrical grid. Aggregation of small energy storage units is considered in [24], the equivalent power and energy capacities can be analytically determined, and an online disaggregation control strategy is suggested. In [25], the flexibility of district heating system is quantified by a three-stage method. In [26], a thermal inertial aggregation model for district heating network is provided to analyze the coupled energy systems. By considering network reduction method for heating system aggregation, a two-stage robust model in [27] is proposed for integrated electricity-heat scheduling to handle electricity and heat uncertainties. This class mainly addresses the multi-scale feature and alleviates the dilemma between system-level decision-making in which tractability is the primary concern and device-level decision-making in which accuracy is the main target.

TABLE I
LITERATURE REVIEW

		Category				
		First	Second	Third	Fourth	Proposed
Dispatch mode	Centralized	✓	✓			
	Horizontal			✓		✓
	Vertical				✓	
Optimization method	Deterministic	✓		✓	✓	
	Two-stage		✓	✓	✓	
	Multistage		✓			✓

The integration of heating and power systems creates both opportunities and challenges in system operation. On the one hand, generation and demand in the power grid must be balanced in real time. With the help of large capacity TES, electric heaters can act as adjustable power demands, so the power grid has some freedom to maintain balance and network constraints. On the other hand, the thermal storage level dynamics create inter-temporal constraints, so the operation problem comes down to a multi-period optimization which requires renewable power and load forecasts. The challenges are twofold: first, prediction is usually inaccurate, especially for renewable power; second, the power and heating systems are monitored by different entities; neither of them possesses the data and model of the other system. To unleash the synergy, a thorough coordination is needed without complicated communication. However, it is difficult to estiblish a whole optimization problem, regardless of how uncertainty is modeled due to the lack of integral system data. Existing methods on the dispatch of interdependent heat-power systems either address uncertainty in a centralized scheme or develop distributed dispatch algorithms while adopting simplified assumptions on uncertainty. This paper addresses the above two challenges in a holistic approach. The proposed method and four existing approaches are compared in Table I which clearly shows their different focuses.

This paper considers the operation of interdependent power distribution network and district heating network. The two systems have similar sizes and are connected through multiple electric heaters. So we do not consider the aggregation problem in the last class, which happens at different spatial scales. We assume the two systems have reached certain agreements, such that the heating system would like to cooperate with the electricity system and provide flexibility, but they do not share private information. The only data exchange is the power demand of electric heaters. The framework belongs to the third class, but we consider multi-period dispatch and the policy is non-anticipative and thus free of renewable power prediction. The contributions of this paper are twofold:

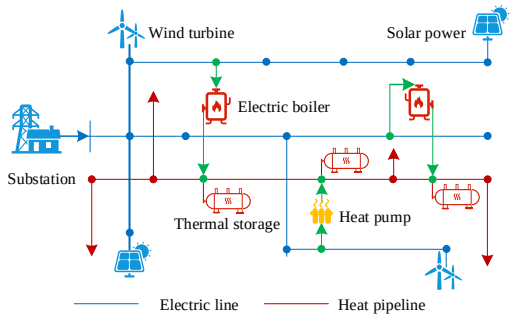

Fig. 1. Interdependent district heating and power distribution networks.

(1) Set-based characterization and quantification of the flexibility from the district heating system. We identify two sets of key variables: the thermal storage levels which bring intertemporal constraints and power demands of electric heaters which couple the two systems. A recursive robust feasibility condition is established for thermal storage levels, ensuring heat supply adequacy under uncertain heat demand. Then, the stagewise robust feasible sets of storage levels are calculated using the polyhedral projection; we propose a customized projection algorithm based on the online vertex enumeration, which is particularly efficient because the dimension of storage level is very low. Finally, dynamic bounds of electric heaters are computed by a further projection step.

(2) An interactive framework for coordinated operation of the integrated distribution system and district heating system. With dynamic bounds of electric heaters that are decoupled over time, the heating system behaves like a flexible demand that can be adjusted in a certain range. This time-decoupled feature allows the distribution system to be operated in response to the real-time information of renewable power, demand, and electricity price without using their forecasts. Nonlinear alternating current power flow model is used in the dispatch. On the contrary, many existing multistage approaches can only handle linear power flow models because the solution procedure involves duality transformation. Unlike distributed algorithms whose efficiency is affected by the convergence rate, in the proposed method, two systems exchange information only once in one period, so there is no convergence issue.

The rest of this paper is organized as follows. The integrated system and energy flow models are introduced in Section II. The set-based formulation of the heating system flexibility and the coordinated operation scheme are developed in Section III. Case study is reported in Section IV. Finally, conclusions are drawn in Section V.

II. System Model

The architecture of the interconnected distribution system and district heating system is introduced first, followed by the energy flow models of respective networks and power-heat conversion of electric heaters.

A. System Configuration

The typical structure of the interconnected system is shown in Fig. 1. Such infrastructure differs from energy hub which is a station-level equipment. In energy hubs, energy conversion and load balancing are the main concerns, while the network structure can be neglected as the system is usually small. In the system shown in Fig. 1, the operation of distribution system and district heating system must obey network constraints, some of which are even nonlinear.

The distribution system connects to a transmission system at a substation, which is the reference node. Electric demands are supplied by the local wind and solar generation which are free of charge. If the renewable power is insufficient, the additional power is purchased from the transmission system at a real-time price ρ_t and delivered from the substation. The value of ρ_t is revealed at the beginning of each period t, and prices in future periods are unknown in advance. Currently, we assume there is no battery storage in the distribution system, so the operation problem boils down to optimal power flow which is naturally decoupled over time. Extensions for including battery are discussed at the end of Section III.

We assume the heating system uses electric heaters, such as electric boilers and heat pumps, although fossil fuel heaters can be considered as well in case of need. Electric heaters connect to different nodes of the distribution system. The heating system possesses several centralized TES units. Since the heating system is willing to provide flexibility in cooperation with the distribution system, we assume electric heaters can use electricity at a constant contract price that is lower than the average retail price. We do not use time-of-use price because it is mainly designed for peak load reduction, while the flexibility offered by the heating system is closer to spinning reserve, whose role is different from peak reduction.

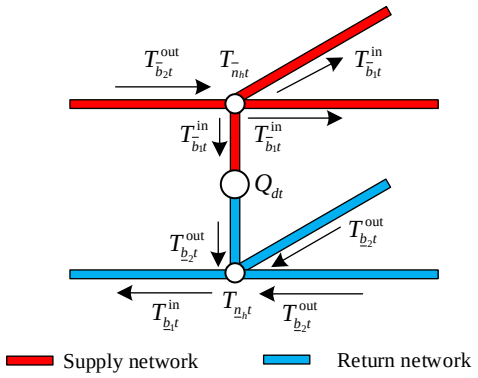

Fig. 2. Pipeline network of the heating system.

B. Heating System Model

The heating system consists of a supply side and a return side. Both sides share the same topology. Heat is supplied by sources and consumed by loads through heat exchangers between the supply side and the return side, as shown in Fig. 2. The heating system is often controlled in the constant-flow variable-temperature mode, under which the supply, demand and nodal temperature obey the following relations [7]

$$c_{\text{p}} m_{[\cdot]} \left(T^{\text{in}}_{[\cdot]t} - T^{\text{out}}_{[\cdot]t} \right) = Q_{[\cdot]t}, \ \forall [\cdot] = h, s, d, \forall t \tag{1a}$$

$$T^{\text{out}}_{bt} = T^{\text{a}}_{t} + e^{-\frac{\lambda L}{c_{\text{p}} m_b}} \left(T^{\text{in}}_{bt} - T^{\text{a}}_{t} \right), \ \forall b, \forall t \tag{1b}$$

$$T^{\text{in}}_{\overline{b}_1 t} = T^{\text{out}}_{\overline{b}_2 t} = T_{\overline{n}_h t},\ \forall \overline{b}_{1,2} \in \overline{\mathcal{N}}_{1,2}, \forall \overline{n}_h, \forall t \tag{1c}$$

$$\sum_{\underline{b}_2 \in \underline{\mathcal{N}}_2} m_{\underline{b}_2} T^{\text{out}}_{\underline{b}_2 t} = \left(\sum_{\underline{b}_1 \in \underline{\mathcal{N}}_1} m_{\underline{b}_1} \right) T^{\text{in}}_{\underline{b}_1 t}, \forall t \tag{1d}$$

$$E_{st} = E_{st-1} + Q_{st}\Delta_t, \forall s, \forall t \tag{1e}$$

$$E^{\min}_s \le E_{st} \le E^{\max}_s, \forall s, \forall t \tag{1f}$$

$$Q^{\min}_{[\cdot]} \le Q_{[\cdot]t} \le Q^{\max}_{[\cdot]},\ \forall [\cdot] = h, s, \forall t \tag{1g}$$

$$T^{\min}_{n_h} \le T_{n_h t} \le T^{\max}_{n_h},\ \forall n_h, \forall t \tag{1h}$$

where $\overline{n}_h/\underline{n}_h$ is the index of nodes at the supply/return side, h, s, d, and b are indices of electric heaters, TES units, loads and pipelines, respectively, t is the index of the period, and Δ_t is the duration of period t. The mass flow rate, thermal energy exchange, and temperature are represented by $m_{[\cdot]}$, $Q_{[\cdot]t}$ and $T_{[\cdot]t}$, respectively, and the superscript in/out associates with a pipeline denotes its inlet and outlet; T^{a}_t is the ambient temperature, c_{p} is the specific heat capacity of water, λ and L are the heat loss coefficient and the length of a pipeline. TES unit is assumed to be lossless, and E_{st} is its storage level.

Constraint (1a) describes the heat exchange in sources, loads and TES units, where $m_{[\cdot]}$ is constant; constraint (1b) reflects the energy loss in pipelines; at the supply side, taking Fig. 2 for an example, fluid in red pipelines diverges at a node and flows into downstream pipelines and a heat exchanger; the temperature does not change at the diverging point as in (1c), where $\overline{\mathcal{N}}_1/\overline{\mathcal{N}}_2$ is the set of pipelines whose inlet/outlet connects to the node $\overline{n}_h$; by the conservation law, mass flow rates at a diverging point must satisfy $\sum_{\overline{b}_1 \in \overline{\mathcal{N}}_1} m_{\overline{b}_1} = m_{\overline{b}_2}$; at the return side, fluid in blue pipelines with different temperatures meets at some nodes, the temperature at the junction node is given in (1d) according to energy conservation law, where $\underline{\mathcal{N}}_1/\underline{\mathcal{N}}_2$ is the set of pipelines whose inlet/outlet connects to the node $\underline{n}_h$, and the mass flow rates at a junction point satisfy $m_{\underline{b}_1} = \sum_{\underline{b}_2 \in \underline{\mathcal{N}}_2} m_{\underline{b}_2}$; in the heat exchanger (represented by the vertical line with demand Q_{dt}), $m_{\overline{b}_1} = m_{\underline{b}_2} = m_d$; the dynamic of thermal storage level is stipulated in (1e); thermal storage level, heat consumption and nodal temperature bounds are summarized in (1f), (1g) and (1h), respectively. The heat load Q_{dt} is a constant here, but will become uncertain in the subsequent section.

C. Distribution System Model

Distribution networks are often operated under radial topology, and the branch flow model in [28] is adopted to formulate power flow equations

$$P_{l_{ij}t} - r_{l_{ij}} I_{l_{ij}t} + p^{\text{in}}_{jt} = \sum\nolimits_{k \in \delta(j)} P_{l_{jk}t} \tag{2a}$$

$$Q_{l_{ij}t} - x_{l_{ij}} I_{l_{ij}t} + q^{\text{in}}_{jt} = \sum\nolimits_{k \in \delta(j)} Q_{l_{jk}t} \tag{2b}$$

$$v_{jt} = v_{it} - 2(r_{l_{ij}} P_{l_{ij}t} + x_{l_{ij}} Q_{l_{ij}t}) + I_{l_{ij}t} z^2_{l_{ij}} \tag{2c}$$

$$\left\| \begin{matrix} 2P_{l_{ij}t} \\ 2Q_{l_{ij}t} \\ I_{l_{ij}t} - v_{it} \end{matrix} \right\|_2 \le I_{l_{ij}t} + v_{it} \tag{2d}$$

$$p^{\min}_{jt} \le p^{\text{in}}_{jt} \le p^{\max}_{jt},\ q^{\min}_{jt} \le q^{\text{in}}_{jt} \le q^{\max}_{jt} \tag{2e}$$

$$v^{\min}_j \le v_{jt} \le v^{\max}_j \tag{2f}$$

where l_{ij} is the index of the distribution line from bus i to bus j; $\delta(j)$ is the set of nodes which connect to the node j through some line; $r_{l_{ij}}/x_{l_{ij}}$ denotes resistance/reactance of a line, and $z^2_{l_{ij}} = r^2_{l_{ij}} + x^2_{l_{ij}}$; $P_{l_{ij}t}/Q_{l_{ij}t}$ is the active/reactive power in a line; $I_{l_{ij}t}$ and v_{it} are the squared line current and the bus voltage; $p^{\text{in}}_{jt} = p^g_{jt} - p^d_{jt} - p^h_{jt}$ ($q^{\text{in}}_{jt} = q^g_{jt} - q^d_{jt}$) is the net active (reactive) power injection at the node j, which is equal to generation minus demand.

In the nodal-wise power balancing condition (2a)-(2b), if there is no generation and load at the node j, then $p^{\text{in}}_{jt} = q^{\text{in}}_{jt} = 0$ is imposed. For conventional units, active power p^g_{jt} and reactive power q^g_{jt} are decision variables subject to capacity limits; for renewable generation, the upper bound of p^g_{jt} depends on the time-varying weather condition and is observed at the beginning of period t, while its lower bound is 0 which means renewable curtailment is allowed. Behind-the-meter resources add uncertainty to the active/reactive power demand p^d_{jt}/q^d_{jt}, which is also revealed before dispatch action is deployed. For the demand p^h_{jt} of electric heaters, the feasible set reflects the flexibility of the heating system and will be discussed in the next section. Fossil fuel generators can also be included in (2), whose minimum/maximum output is constant.

For the remaining constraints, voltage drop along a distribution line is expressed in (2c); the apparent power injection at the head node of a line satisfies $I_{l_{ij}t} v_{it} = P^2_{l_{ij}t} + Q^2_{l_{ij}t}$ which defines a non-convex set; it is known that replacing this equality with an inequality $I_{l_{ij}t} v_{it} \ge P^2_{l_{ij}t} + Q^2_{l_{ij}t}$, which is called the second-order cone relaxation as applied in (2d), does not influence the optimal solution under mild conditions [29]; constraints (2e)-(2f) limits the active/reactive power injection as well as the squared nodal voltage.

D. Electric Heaters

Electric heaters are modeled through a power-heat conversion equality

$$Q_{h_j t} = \kappa_h p^h_{jt} \tag{3}$$

On the righthand side of (3), p^h_{jt} is the power demand of heater appeared in the power balance condition; on the lefthand side of (3), $Q_{h_j t}$ is the output of the heater connect to node j in the distribution system; κ_h is the conversion efficiency of electric heaters h. For electric boilers, κ_h is close to 1 [30]; for heat pumps, κ_h is known as the coefficient of performance, which is 3-4 for the air-source type [31] and 4-5 for the ground-source type [32].

Energy conversion from heat to electricity is not considered, because the district heating system is used for room heating, and the heat transfer fluid is hot water at a temperature of 90-100 centigrade. The low-temperature heat is not suitable for electricity generation due to the low Carnot efficiency.

III. Proposed Method

The basic theory and computational implementation of the proposed method are presented in three subsections. In the last subsection, the coordinated dispatch method is developed.

A. Recursive Robust Feasibility Condition

The network models in Section II are static; the only inter-temporal constraint originates from the storage level dynamic equation (1e). As the capacity of the TES unit is finite, the current dispatch of TES unit affects how it can be used in the future. The key component to ensure supply adequacy in the heating system under the uncertain heat demand is to monitor the thermal storage level.

The uncertainty of heat demand is caused by many factors, such as outdoor temperature and user comfortable preference. We assume Q_{dt} may vary in a certain interval, so the uncertainty set $\mathcal{U}_t$ of heat demands $Q_{[d]t} = [Q_{dt}], \forall d$ in the period t is a hypercube

$$\mathcal{U}_t = \left\{ Q_{[d]t} \middle| \underline{Q}_{dt} \le Q_{dt} \le \overline{Q}_{dt}, \forall d \right\} \quad \forall t \tag{4}$$

Next, heating system constraints in (1) are cast in a compact form. To shorten symbols in theoretical development, variables are divided into three categories: (a) the state variable $x_t = [E_{st}], \forall s$ includes thermal storage level which produces inter-temporal constraints; (b) the uncertain parameter $Q_{[d]t}$; (c) the non-state variable y_t includes all other variables in the period t. Under a constant-flow control mode, the mass flow rate $m_{[\cdot]}$ is fixed, and constraints in (1) are linear. With the above notations, the feasible set defined by (1) can be rewritten as

$$\mathcal{F}_t = \left\{ (x_{t-1}, x_t, y_t, Q_{[d]t}) \middle| \begin{matrix} Ax_{t-1} + Bx_t \\ + Cy_t + DQ_{[d]t} \le a_t \end{matrix} \right\} \tag{5}$$

where A, B, C, D, a_t are constants corresponding to the coefficients in (1). At the beginning of period t, the values of storage level x_{t-1} and heat demand $Q_{[d]t}$ become apparent, and the feasible set of (x_t, y_t) is

$$\mathcal{F}_t(x_{t-1}, Q_{[d]t}) = \left\{ (x_t, y_t) \middle| \begin{matrix} Bx_t + Cy_t \le \\ a_t - Ax_{t-1} - DQ_{[d]t} \end{matrix} \right\} \tag{6}$$

Considering the uncertainty of heat demand, the state variable x_t in every period must be carefully chosen in order to fulfill a feasible operation of the heating system. The difficulty arises from the time-coupling feature of the constraint (1e). We must quantify how x_t affects the feasibility of future stages.

Consider the problem backward. In the period t, a necessary and sufficient condition to warrant the robust feasibility under the heat demand uncertainty $Q_{[d]t} \in \mathcal{U}_t$ is to select x_{t-1} in a one-step lookahead manner such that

$$\forall Q_{[d]t} \in \mathcal{U}_t : \mathcal{F}_t(x_{t-1}, Q_{[d]t}) \ne \emptyset \tag{7}$$

The condition (7) guarantees the existence of some dispatch actions (x_t, y_t) satisfying all constraints in (1), regardless of the value of $Q_{[d]t}$ as long as it remains in $\mathcal{U}_t$. However, the condition (7) cannot ensure feasibility in period $t+1$ and later. Nevertheless, this condition provides some insights:

(a) The impact of the uncertainty can be taken into account by investigating all possible outcomes;
(b) The condition (7) actually imposes additional constraints on the state variable in period $t-1$. Though the condition in (7), we obtain higher robustness in the period t through sacrificing the flexibility in the period $t-1$.

To develop a prediction-free operation method for the coupled systems, two problems need further investigations. First, the condition (7) contains infinitely many constraints as it entails an enumeration over $\mathcal{U}_t$. How can we reduce this condition to a tractable one? Second, although condition (7) is responsible for the feasibility in the period t, it overlooks the feasibility in period $t+1$ and later. How can we extend it to a multistage optimization problem?

For the first problem, because $\mathcal{U}_t$ is a convex set, we can replace $\mathcal{U}_t$ with its vertex set $\text{vert}(\mathcal{U}_t) = \{Q_{[d]t}^{v_1}, \cdots, Q_{[d]t}^{v_K}\}$. To see this, let $(x_t^{v_1}, y_t^{v_1}), \cdots, (x_t^{v_K}, y_t^{v_K})$ be the corresponding feasible solutions, which means that

$$\begin{gathered} Ax_{t-1} + Bx_t^{v_1} + Cy_t^{v_1} + DQ_{[d]t}^{v_1} \le a_t \\ \vdots \\ Ax_{t-1} + Bx_t^{v_K} + Cy_t^{v_K} + DQ_{[d]t}^{v_K} \le a_t \end{gathered}$$

Any $Q_{[d]t} \in \mathcal{U}_t$ can be expressed via the convex combination

$$Q_{[d]t} = \lambda_1 Q_{[d]t}^{v_1} + \cdots + \lambda_K Q_{[d]t}^{v_K}$$

where $\lambda_1, \cdots, \lambda_K \ge 0$ and $\sum_{i=1}^K \lambda_i = 1$. Multiplying both sides of the above K linear inequalities by the K weights and then adding them together, we have

$$Ax_{t-1} + B\sum_{i=1}^K \lambda_i x_t^{v_i} + C\sum_{i=1}^K \lambda_i y_t^{v_i} + DQ_{[d]t} \le a_t$$

This means that $(\sum_{i=1}^K \lambda_i x_t^{v_i}, \sum_{i=1}^K \lambda_i y_t^{v_i}) \in \mathcal{F}_t(x_{t-1}, Q_{[d]t})$, so $\mathcal{F}_t(x_{t-1}, Q_{[d]t}) \ne \emptyset$, and the condition in (7) is satisfied. Hence, the enumeration over $\mathcal{U}_t$ and $\text{vert}(\mathcal{U}_t)$ has the same effect, but the latter one is a finite set.

For the second problem, from the observation in item (b), we know robustness can be obtained by adding constraints on state variables. Assume we have obtained the analytical form of these robustification constraints, denoted by $\mathcal{X}_t$, then we can extend the condition (7) in a recursive way:

$$\mathcal{X}_{t-1} = \left\{ x_{t-1} \middle| \begin{matrix} \forall Q_{[d]t} \in \text{vert}(\mathcal{U}_t) \\ \exists (x_t \in \mathcal{X}_t, y_t) : \\ \mathcal{F}_t(x_{t-1}, Q_{[d]t}) \ne \emptyset \end{matrix} \right\}, \ t = 2 : T \tag{8}$$

where $\mathcal{X}_t, t = 1 : T$ are called **stagewise robust feasible sets** of thermal storage level. If we have $\mathcal{X}_T$ in the last period, we can find $\mathcal{X}_{T-1}$, then $\mathcal{X}_{T-2}$, and finally $\mathcal{X}_1$ based on the condition (8). The calculation of sets $\mathcal{X}_1, \cdots \mathcal{X}_{T-1}$ depends on their polyhedral property and is left to the next subsection.

B. Computation of Stagewise Robust Feasible Sets

A fundamental concept used in the following discussion is polyhedral projection. Consider a bounded polyhedron

$$\mathcal{P} = \{(x, y) \mid Ax + By \le b\}$$

where $x \in \mathbb{R}^l$ and $y \in \mathbb{R}^n$ are variables, and matrices A, B and vector b have compatible dimensions for multiplication. The projection of $\mathcal{P}$ onto the subspace spanned by the first l dimensions is denoted by

$$\text{Proj}_{[1:l]}(\mathcal{P}) = \{x \mid \exists y : By \le b - Ax\} \tag{9}$$

The definition in (9) can be viewed as the dimension reduction via eliminating the variable y. It is proven in [33] that the projected set can be expressed as

$$\mathrm{Proj}_{[1:l]}(\mathcal{P}) = \left\{x \mid u^\top Ax \geq u^\top b,\ \forall u \in \mathrm{vert}(U)\right\} \quad (10)$$

where $\mathrm{vert}(U)$ represents all the vertices of polytope

$$U = \left\{u \mid B^\top u = 0,\ -1 \leq u \leq 0\right\}$$

From (10) we can see that the projected set $\mathrm{Proj}_{[1:l]}(\mathcal{P})$ in (9) remains a polyhedron since $\mathrm{vert}(U)$ has finite elements.

Typically, projection can be calculated by Fourier-Motzkin elimination. For a dense system with ℓ linear inequalities, Fourier-Motzkin elimination method introduces $\ell^2/4$ new linear inequalities after eliminating one variable in the worst case, and most of them are redundant. For the problem considered in this paper, the majority of variables are to be eliminated, and only a few variables are left. In other words, the dimension l of the target space is low, and $n \gg l$. For such kind of problem, we propose a customized projection algorithm based on formula (10). However, because B is a high dimensional matrix, vertex enumeration is not viable. We only need to find out those vertices that define the boundary of $\mathcal{X}_{t-1}$.

To this end, we consider a problem: given a polytope $\mathcal{X}$, certify $\mathcal{X} \subseteq \mathrm{Proj}_{[1:l]}(\mathcal{P})$ or find some $x \in \mathcal{X}$ but x is not an element of $\mathrm{Proj}_{[1:l]}(\mathcal{P})$, which is called a separation oracle. According to (10), if $\mathcal{X} \subseteq \mathrm{Proj}_{[1:l]}(\mathcal{P})$ is true, there must be

$$u^\top Ax \geq u^\top b,\ \forall u \in U,\ \forall x \in \mathcal{X}$$

Because (10) is an exact expression, if $\exists x \notin \mathrm{Proj}_{[1:l]}(\mathcal{P})$, there must be some vertices $u^\star \in U$ such that $(u^\star)^\top Ax < (u^\star)^\top b$, so the hyperplane

$$(u^\star)^\top Ax \geq (u^\star)^\top b \quad (11)$$

strictly separates x from $\mathrm{Proj}_{[1:l]}(\mathcal{P})$, and this constraint will not remove any point inside $\mathrm{Proj}_{[1:l]}(\mathcal{P})$ because of (10).

Given the above analysis, the strategy for computing the projected set is to firstly create a large enough initial set $\mathcal{X}$ that contains the projected set, and then gradually remove the unqualified region by creating cutting planes, until the separation oracle gives a positive certification, which entails solving the following bilinear program:

$$\begin{aligned} R = \max\ & u^\top(b - Ax) \\ \text{s.t.}\ \ & u \in U,\ x \in \mathcal{X} \end{aligned} \quad (12)$$

Since $u = 0$ is always feasible in U, the optimal value R must be non-negative. If $R = 0$, then (10) is certified and the current set $\mathcal{X}$ is the projection set. Otherwise, if $R > 0$, a cutting plane (11) is generated using the current optimal solution $u^\star$.

However, the problem (12) is non-convex. To find the global optimum, it is transformed into a mixed-integer linear program in [33]. Here we propose a linear programming based method to solve problem (12) much more efficiently. An important property of the problem (12) is that its optimal solution must be found at a pair of vertices of U and $\mathcal{X}$ [34]. Based on this property, if the vertex set $\mathrm{vert}(\mathcal{X}) = \left\{x^1, \cdots, x^K\right\}$ is available, then we solve K linear programs

$$R_k = \max\left\{u^\top(b - Ax^k) : u \in U\right\},\ k = 1:K \quad (13)$$

and $R = \max_k\{R_k\}$. Because $\dim(\mathcal{X}) = l$ which is usually no larger than 10, the vertex enumeration for $\mathcal{X}$ is easy. Actually, in each step, only one hyperplane in form of (11) is added into $\mathcal{X}$. It removes some old vertices and intersects with some edges of $\mathcal{X}$ and thus generates some new vertices. We just need to track the change in a small fraction of elements in the vertex set, which is implemented by the online vertex enumeration algorithm in [35]. Therefore, only a few linear programs are solved in each iteration. The flowchart of computing the set $\mathrm{Proj}_{[1:l]}(\mathcal{P})$ is provided in Algorithm 1.

Algorithm 1 : Customized Polyhedral Projection

1: Initiate $\mathcal{X}^{\mathrm{B}} = \left\{x_t \mid E_s^{\min} \leq E_{st} \leq E_s^{\max}, \forall s\right\}$ and set an error tolerance $\delta > 0$;
2: Solve the problem (12) through linear programs corresponding to those vertices of the current $\mathcal{X}^{\mathrm{B}}$. The optimal solution is $(u^\star, x^\star)$, and the optimal value is R.
3: If $R \leq \delta$, terminate and report the current $\mathcal{X}^{\mathrm{B}}$ as the projection set; otherwise, add a cutting plane (11) to $\mathcal{X}^{\mathrm{B}}$.
4: Update $\mathcal{X}^{\mathrm{B}}$ and its vertex set using the online vertex generation method in [35]. Return to step 2.

With the above knowledge, we can show the polyhedral property of $\mathcal{X}_1, \cdots, \mathcal{X}_T$ and calculate their hyperplane representations using the backward induction. In the last stage T, there is no future period, and $\mathcal{X}_T$ is the physical bound of thermal storage level, which is a hypercube

$$\mathcal{X}_T = \left\{x_T \mid E_s^{\min} \leq E_{sT} \leq E_s^{\max}, \forall s\right\}$$

Assume in the period t, the stagewise feasible set $\mathcal{X}_t$ of the state variable x_t can be calculated and remains a polyhedral set, then in the period $t-1$, by the condition in (8) we have

$$\mathcal{X}_{t-1} = \left\{ x_{t-1} \middle| \begin{array}{l} \forall Q_{[d]t}^{v_i} \in \mathrm{vert}(\mathcal{U}_t),\ \exists (x_t^{v_i} \in \mathcal{X}_t, y_t^{v_i}) : \\ Bx_t^{v_i} + Cy_t^{v_i} + DQ_{[d]t}^{v_i} \leq a_t - Ax_{t-1} \end{array} \right\} \quad (14)$$

Because $\mathrm{vert}(\mathcal{U}_t)$ has finite elements, $\mathcal{X}_t$ is polyhedral, and the number of inequality constraints in (14) is finite, the set

$$\mathcal{P}_{t-1}(\mathcal{U}_t) = \left\{ \begin{bmatrix} x_{t-1} \\ (x_t^{v_i}, y_t^{v_i}), \forall v_i \end{bmatrix} \middle| \begin{array}{l} Ax_{t-1} + Bx_t^{v_i} + Cy_t^{v_i} \leq \\ a_t - DQ_{[d]t}^{v_i}, x_t^{v_i} \in \mathcal{X}_t, \forall v_i \end{array} \right\}$$

depending on $\mathcal{U}_t$ is a polytope, where v_i is the index of vertices in $\mathrm{vert}(\mathcal{U}_t)$. Assume the dimension of state variable is m, by definition (9), $\mathcal{X}_{t-1}$ can be expressed via projection as

$$\mathcal{X}_{t-1} = \mathrm{Proj}_{[1:m]}(\mathcal{P}_{t-1}(\mathcal{U}_t)) \quad (15)$$

According to the property of the projection operator, the output $\mathcal{X}_{t-1}$ remains a polyhedron [36]. Finally, by the principle of induction, $\mathcal{X}_1, \cdots, \mathcal{X}_T$ are all polyhedral sets.

The above discussions not only demonstrate the polyhedral structure of stagewise robust feasible sets $\mathcal{X}_1, \cdots, \mathcal{X}_T$, but also construct their hyperplane expressions. With sets $\mathcal{X}_{1:T}$ at hand, the heating system can make online decisions without demand forecast. In period t, thermal storage level x_{t-1} and current heat demand $Q_{[d]t}$ are received; the action set is

$$\mathcal{A}_t = \left\{(x_t, y_t) \mid (x_t, y_t) \in \mathcal{F}_t(x_{t-1}, Q_{[d]t}), x_t \in \mathcal{X}_t\right\} \quad (16)$$

where $\mathcal{F}_t$ originates from operating constraints of the heating system, and $\mathcal{X}_t$ accounts for the feasibility of future stages.

C. Flexibility From the Heating System

At the distribution system side, electric heaters act as power demands, and thermal storage levels are not observable. The power demand from the heating system is flexible because the power consumption of electric heaters has some freedom to be adjusted as long as $(x_t, y_t) \in \mathcal{A}_t$.

To characterize the flexibility from heating system, the non-state variable y_t is further divided into the boundary variable $y_{[h]t} = [Q_{ht}], \forall h$ including outputs of electric heaters and the non-boundary variable y_t^{in} containing all remaining variables in y_t such as the charging and discharging power of TES units. Flexibility refers to the set in which y_t can be adjusted without sacrificing heat supply adequacy of the heating system.

To quantify the flexibility, we work on the action set $\mathcal{A}_t$. Under the help of the stagewise robust feasible set for state variables, $\mathcal{A}_t$ in each stage is decoupled over time with newly observed $(x_{t-1}, Q_{[d]t})$ being the input. Let $y_t = [y_{[h]t}, y_t^{\text{in}}]$, recall the definition in (16) and the expression of $\mathcal{F}_t(x_{t-1}, Q_{[d]t})$ in (6), the action set can be written as

$$\mathcal{A}_t(x_{t-1}, Q_{[d]t}) = \left\{ \begin{bmatrix} y_{[h]t} \\ y_t^{\text{in}} \\ x_t \end{bmatrix} \middle| \begin{array}{l} Bx_t + C^{\text{h}} y_{[h]t} + C^{\text{in}} y_t^{\text{in}} \\ \le a_t - Ax_{t-1} - DQ_{[d]t} \\ x_t \in \mathcal{X}_t \end{array} \right\} \tag{17}$$

where $C = [C^{\text{h}}, C^{\text{in}}]$. The flexibility is given by the feasible set $\mathcal{B}_t^\dagger$ of $y_{[h]t}$ such that $\mathcal{A}_t(x_{t-1}, Q_{[d]t}) \neq \emptyset$. By the definition of projection, we have

$$\mathcal{B}_t^\dagger = \left\{ y_{[h]t} \middle| \exists (x_t, y_t^{\text{in}}) : (y_{[h]t}, y_t^{\text{in}}, x_t) \in \mathcal{A}_t(x_{t-1}, Q_{[d]t}) \right\}$$

Let $\dim(y_{[h]t}) = m'$, then

$$\mathcal{B}_t^\dagger = \text{Proj}_{[1:m']}(\mathcal{A}_t(x_{t-1}, Q_{[d]t}))$$

The projection can be calculated by Algorithm 1. Finally, the output $y_{[h]t}$ of heaters is converted to a power demand $p_t^{[h]}$ via coefficient $\kappa_{[h]}$, and the **flexible loadability set** is defined as

$$\mathcal{B}_t = \left\{ p_t^{[h]} \middle| \kappa_{[h]}^{\text{D}} p_t^{[h]} \in \mathcal{B}_t^\dagger \right\} \tag{18}$$

where $p_t^{[h]} = [p_t^h], \forall h$ collects power demands of heaters, and $\kappa_{[h]}^{\text{D}}$ is a diagonal matrix whose diagonal elements are $\kappa_h, \forall h$. The product $\kappa_{[h]}^{\text{D}} p_t^{[h]}$ is equivalent to let $y_{ht} = \kappa_h p_t^h$ for each heater and then define a vector $y_{[h]t} = [y_{ht}], \forall h$.

To obtain $\mathcal{B}_t$, each dimension of $\mathcal{B}_t^\dagger$ is divided by a factor of κ_h. As $\mathcal{X}_t$ is taken into account in $\mathcal{B}_t$, the operation feasibility of the heating system in the future is guaranteed regardless of the variation of heat demands in the uncertainty set. From the electricity system side, the power consumption $p_t^{[h]}$ of heaters has more freedom and can be adjusted in a polyhedral set $\mathcal{B}_t$. In this regard, heating system can provide flexibility without sacrificing security.

Remark: The increased complexity is a common difficulty of all projection algorithms, because the numbers of vertices and facets grow rapidly in the dimensionality, regardless of how they are computed. In the heating system, the dimension of $\mathcal{X}_t/\mathcal{B}_t$ is equal to the number of large TES units/electric heaters, which is less than 10. User-side distributed devices are combined into heat demand. Consequently, Algorithm 1 remains efficient for practically sized systems.

D. Coordinated Operation of the Interdependent Systems

Now we are ready to present the coordinated operation scheme for the interconnected systems. In the day-ahead stage, the heating system procures the uncertainty set of heat demand $\mathcal{U} = \mathcal{U}_1 \times \cdots \times \mathcal{U}_T$, and then calculates the stagewise robust feasible sets $\mathcal{X}_1, \cdots, \mathcal{X}_T$.

In the real-time operation, at the beginning of the period t, the heating system operator receives the value of $(x_{t-1}, Q_{[d]t})$, then it calculates the flexible loadability set $\mathcal{B}_t$ and submits it to the distribution system. While receiving $\mathcal{B}_t$, the distribution system operator solves an optimal power flow problem

$$\begin{aligned} \min \quad & \rho_t \sum\nolimits_{j \in \delta(0)} P_{0j} \\ \text{s.t.} \quad & \text{branch flow model (2)} \\ & p_t^{[h]} \in \mathcal{B}_t \end{aligned} \tag{19}$$

where ρ_t is the electricity price at node 0; $\delta(0)$ is the set of child nodes of the reference node 0; P_{0j} denotes the active power flow in distribution lines connect to node 0; so the objective function is the cost paid to the transmission system; if gas-fired plant is taken into account, its fuel cost is also added in the objective function; power flow in the distribution system obeys branch flow model in (2); the flexible range of electric heaters are highlighted in the last constraint.

There is no renewable curtailment penalty in the objective function because the waste of solar and wind power is caused by the lack of demand and storage capacity. The optimal dispatch naturally prioritizes the use of free renewable power and is not affected by the penalty, although the objective value would be higher if curtailment is inevitable. The proposed method improves the use of renewable power for two reasons:

(1) The demand of electric heaters are adjustable within the set $\mathcal{B}_t$, so the power grid has some freedom to meet power balance and maintain network constraints.
(2) The thermal storage level are strategically scheduled to circumvent a myopic decision, which is the main shortcoming of greedy policy.

After solving problem (19), the power consumption $p_t^{[h]}$ of electric heaters is sent to the heating system, and then the pipeline network loss is minimized, yielding

$$\begin{aligned} \min_{x_t, y_t^{\text{in}}} \quad & \sum\nolimits_b \left(T_{bt}^{\text{in}} - T_{bt}^{\text{out}} \right) \\ \text{s.t.} \quad & (y_{[h]t}, y_t^{\text{in}}, x_t) \in \mathcal{A}_t(x_{t-1}, Q_{[d]t}) \\ & \text{heater model (3)} \end{aligned} \tag{20}$$

The procedure repeats until the last period T.

The reason of not using a cost as the objective function in (20) is explained as follows. Under a constant pricing scheme, as we have assumed, the daily cost is influenced by the sum of total energy demand and network losses in this day. The former is beyond the control of the heating system operator, and the latter is minimized in (20). Although fixing $p_t^{[h]}$ sacrifices some degree of freedom, considering the fact that loss only accounts for a small fraction of energy, cooperating with the electricity system and thus obtaining a lower electricity price is worthwhile. In summary, the flowchart of the online operation scheme is give in Algorithm 2.

Algorithm 2 : Coordinated Operation Scheme

1: **Day-ahead stage**: initiating uncertainty set $\mathcal{U} = \mathcal{U}_1 \times \cdots \times \mathcal{U}_T$. Let $\mathcal{X}_T = \left\{x_T \mid E_s^{\min} \le E_{sT} \le E_s^{\max}, \forall s\right\}$
For $t = T-1:1$
Compute $\mathcal{X}_t$ according to (15) based on Algorithm 1.
End

2: **Real-time stage**:
For $t = 1:T$
- Heating system observes $(x_{t-1}, Q_{[d]t})$, calculates $\mathcal{B}_t$ in (18) based on Algorithm 1, then submits $\mathcal{B}_t$ to the distribution system;
- Distribution system receives $\mathcal{B}_t$ and solves problem (19), and then sends $p_t^{[h]}$ to the heating system;
- Heating system receives $p_t^{[h]}$ and then solves problem (20). Proceed to the next period.

End

E. Extensions for the Inclusion of Battery Storage

If battery storage is deployed in the distribution system, the proposed method can also be applied. Two situations are considered depending on the rated charging time $T_{\mathrm{r}}^{\mathrm{B}} = E_{\mathrm{B}}^{\max}/p_{\mathrm{B}}^{\max}$ of the battery, where $E_{\mathrm{B}}^{\max}$ is the energy capacity in MWh; $p_{\mathrm{B}}^{\max}$ is the maximum charging power in MW.

(1) If $T_{\mathrm{r}}^{\mathrm{B}} \le 2$ hours, applying greedy policy amounts to adding bound constraints

$$0 \le p_t^{\mathrm{ch}} \le \min\left\{\frac{E_{\mathrm{B}}^{\max} - E_{t-1}^{\mathrm{B}}}{\eta_{\mathrm{ch}}^{\mathrm{B}}\Delta_t}, p_{\mathrm{B}}^{\max}\right\} \tag{21a}$$

$$0 \le p_t^{\mathrm{dc}} \le \min\left\{\frac{(E_{t-1}^{\mathrm{B}} - E_{\mathrm{B}}^{\min})\eta_{\mathrm{dc}}^{\mathrm{B}}}{\Delta_t}, p_{\mathrm{B}}^{\max}\right\} \tag{21b}$$

to the OPF problem (19), where E_{t-1}^{B} is the battery storage level at the end of period $t-1$, which is a known constant at the beginning of period t; $\eta_{\mathrm{ch}}^{\mathrm{B}}/\eta_{\mathrm{dc}}^{\mathrm{B}}$ is charging/discharging efficiency; $p_t^{\mathrm{ch}}/p_t^{\mathrm{dc}}$ is battery charging/discharging power, bounded by $p_{\mathrm{B}}^{\max}$. At the end of period t, the battery storage level is changed to

$$E_t^{\mathrm{B}} = E_{t-1}^{\mathrm{B}} + \eta_{\mathrm{ch}}^{\mathrm{B}} p_t^{\mathrm{ch}}\Delta_t - p_t^{\mathrm{dc}}\Delta_t/\eta_{\mathrm{dc}}^{\mathrm{B}}$$

The constraint $E_{\mathrm{B}}^{\min} \le E_t^{\mathrm{B}} \le E_{\mathrm{B}}^{\max}$ is always warranted by the constraints in (21), so battery storage level E_t^{B} and its dynamic equation are omitted. In a cost minimization problem, p_t^{ch} and p_t^{dc} at the optimal solution is complementary, because simultaneous charging and discharging incur losses and thus not optimal [37].

(2) If $T_{\mathrm{r}}^{\mathrm{B}} > 2$ hours or it is comparable to the rated charging time of TES, the proposed method for heating system can be applied again to the distribution system, and then the inter-temporal constraints of battery storage are decomposed. In this case, the day-ahead problem adopts a linear power flow model, such as the linearized distflow model in [38], because Algorithm 1 must be performed with linear constraints. If a nonlinear power flow model is preferred, the polyhedral approximation method in [39] can be applied. Therefore, to include battery storage, the accuracy of power flow model in the day-ahead stage is slightly sacrificed, but we can still use the nonlinear power flow model in the real-time stage. It is known that the linearized distflow model has satisfactory accuracy, so the discrepancy would not be significant.

F. Connection with Multistage Robust Optimization

The classic multistage robust optimization belongs to the category of centralized optimization, which is often solved by the dynamic programming type algorithms. However, because the heating and power systems are monitored by different entities and there lacks a holistic model, a centralized approach is difficult to implement. Algorithm 2 can be regarded as a distributed scheme to a special multistage robust optimization problem. However, there are three significant differences.

1) We develop a set-based decomposition algorithm to break the temporal dependency brought by thermal storage dynamics. The dynamic programming method based on Bellman's Principle of Optimality constructs optimal value functions in each period recursively, while the proposed method offers feasible sets in each stage; the recursive equation (8) plays the similar role as Bellman's equation, but from the perspective of feasibility instead of optimality. The economic issue is taken into account in the real-time stage via optimal power flow. This paradigm is suitable in power system operation where cost is to be minimized subject to mandatory security constraints.

2) The stagewise robust feasible set of state variables breaks the temporal dependency brought by thermal storage dynamics; the flexible loadability set of coupling variables breaks the interdependency across the two systems and allow them to be operated in a distributed manner. Both sets have clear physical meanings. The existing multistage robust optimization requires a centralized model, which encounters difficulties in practice as neither of the two systems have complete model and data of the integral network.

3) To develop computationally tractable algorithms, existing multistage robust optimization usually relies on linear mathematical models. In contrast, with the flexible loadability set from the heating system, the power system operation can be optimized according to the AC power flow model, which is more accurate than the linearized power flow models and hence preferred in practical usage.

IV. Case Study

The performance of the proposed method is examined on two testing systems of different scales. The small system is comprised of a 33-bus distribution network and a 14-node heating network. The large one consists of a modified 123-bus distribution system and a 45-node heating system. The algorithms are coded in Julia environment, optimization problems are solved by Gurobi. All numerical tests are conducted on a laptop with Intel i7-10710U CPU and 16GB RAM.

A. Results for the Small System

The structure of this system is shown in Fig. 3. In the 33-bus distribution system, 4 wind turbines and 3 solar plants are connected. The 14-node heating network possesses 2 electric boilers, 1 heat pump and 3 TES units. Complete system data can be found in [40]. The day-ahead interval forecasts of heat

demands are plotted in Fig. 4, which serves as the uncertainty set. The observed trajectory of heat demands is also shown in Fig. 4. The dispatch interval is $\Delta_t = 1$ hour.

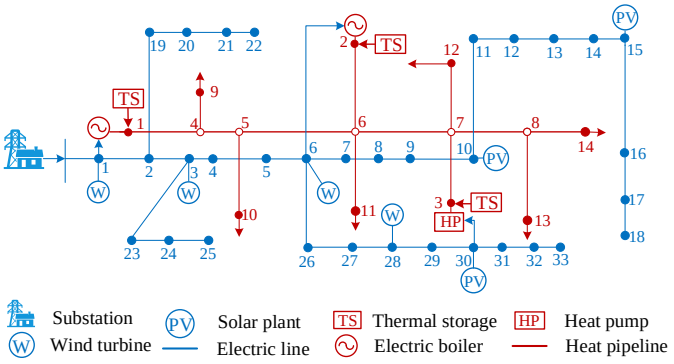

Fig. 3. Topology of the small testing system.

1) Sets Visualization: In this case, the dimension of x_t is 3, so we can visualize $\mathcal{X}_{1:24}$ in $\mathbb{R}^3$. The most popular projection algorithm is Fourier-Motzkin elimination. It fails to offer a result in one hour. For Algorithm 1, the polytope resides in $\mathbb{R}^3$, so the vertex update in step 4 is very efficient, and the bilinear program (12) can be easily solved. In consequence, Algorithm 1 takes only 470 seconds to calculate all stagewise robust feasible sets $\mathcal{X}_{1:24}$ which are plotted in Fig. 5. Because the heat demand is high during periods 5-13, some part around the corner corresponding to the minimum storage level in $\mathcal{X}_{4:12}$ is cut off in periods 4-12, which is one period earlier than the peak demand arrives, to maintain thermal storage at the sufficiently high level. Due to the charging power capacity of the TES, the minimum storage level cannot be reached immediately in period 4, so the TES is charged in advance during periods 2-3. In remaining periods, $\mathcal{X}_t = \mathcal{X}_{24}$.

Dynamic bounds $\mathcal{B}_{1:24}$ of electric heaters are calculated, consuming 39 seconds. They are drawn in Fig. 6. Take $\mathcal{B}_2$ in the period 2 for example, it consists of 30 vertices and 17 facets. As the thermal storages level in the period 1 is sufficiently high to provide flexibility and the heat demand in the period 3 is moderate, there is no need to maintain a very high storage level in the period 2. As a result, $\mathcal{X}_2$ and $\mathcal{B}_2$ are relatively large compared to those in periods 3-12.

2) Operation Methods for Comparison: The proposed method is compared with three competitors. The details can be found in the appendix.

Hindsight optimum: Assume the coupled systems is centrally operated. At the end of a day, the heat demand data is known exactly. The hindsight optimum refers to the optimal value of a deterministic problem with known heat demand trajectory. Although the ideal hindsight optimum cannot be acheived in practice, it offers a baseline to quantify the optimality performance of other online policies.

Centralized greedy method: Still in a centralized scheme, the greedy policy π_G makes a decision based on the current observation of the uncertainty and thermal storage levels.

Hierarchical MPC: In this scheme, the heating system predicts heat demands in the next 24 hours and solves a minimum loss problem, then submits power demands of heaters in the current period to the distribution system. The dispatch actions can be retrieved from the optimal power flow solution. This policy is denoted by π_M.

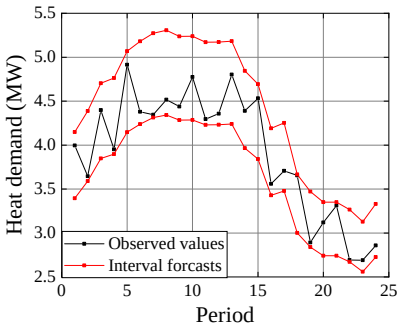

Fig. 4. Interval forecasts and observed values of heat demands.

3) Overall Performance Comparison: The proposed policy in Algorithm 2, denoted by π_{OL}, is compared with π_G and π_M over a period of 4 months from November to February, covering the heating period in most areas of northern China. Results are shown in Table II.

Given exact heat demands in the next day, the hindsight problem (22) (see appendix) in each day of four months is solved, and the minimum cost is $f^* = 4.87 \times 10^5$\$. All other policies incur higher costs compared to this benchmark. In the hierarchical MPC policy, using exact heat demand forecasts, the heating system solves the minimum loss problem (24) and submits demands of electric heaters to the distribution system. Since there is no forecast error, such a strategy is ideally optimal to the heating system. Then, the distribution system executes dispatch according to the optimal power flow problem (25). Unlike problem (19) where the power demand $p_t^{[h]}$ is adjustable in the set $\mathcal{B}_t$, $p_t^{[h]}$ is fixed in problem (25), making the dispatch of distribution system less flexible. As a result, π_M incurs a total cost of 5.39×10^5\$, which is 10.68% higher than f^*.

The proposed method does not rely on exact heat demand forecasts. Instead, it uses interval forecasts in the day-ahead stage to construct robust feasible sets and flexible loadability sets. Taking industrial experiences into account, the day-ahead forecast error is assumed to be 10%, and the resulting $\mathcal{X}_{1:24}$ and $\mathcal{B}_{1:24}$ in a typical day have been shown in Figs. 5-6. In the real-time stage, the optimal power flow problem (19) is a second-order conic program, and the optimal thermal flow problem (20) is a linear program. Both of them can be solved in less than a second, so the computation time can be neglected. In the heat supply period of 4 months, the proposed policy π_{OL} receives a total cost of 4.98×10^5\$, which is 2.26% higher than the ideal optimum f^* but much better than that of π_M. One reason can be seen from the last column: renewable energy curtailment rate under π_{OL} is lower compared to that under π_M, so less electricity is purchased from the transmission system, leading to a lower total cost. The relative power procurement, which is equal to the import power under some policy π minus that under the hindsight optimal solution, is shown in Fig. 7. Because TES

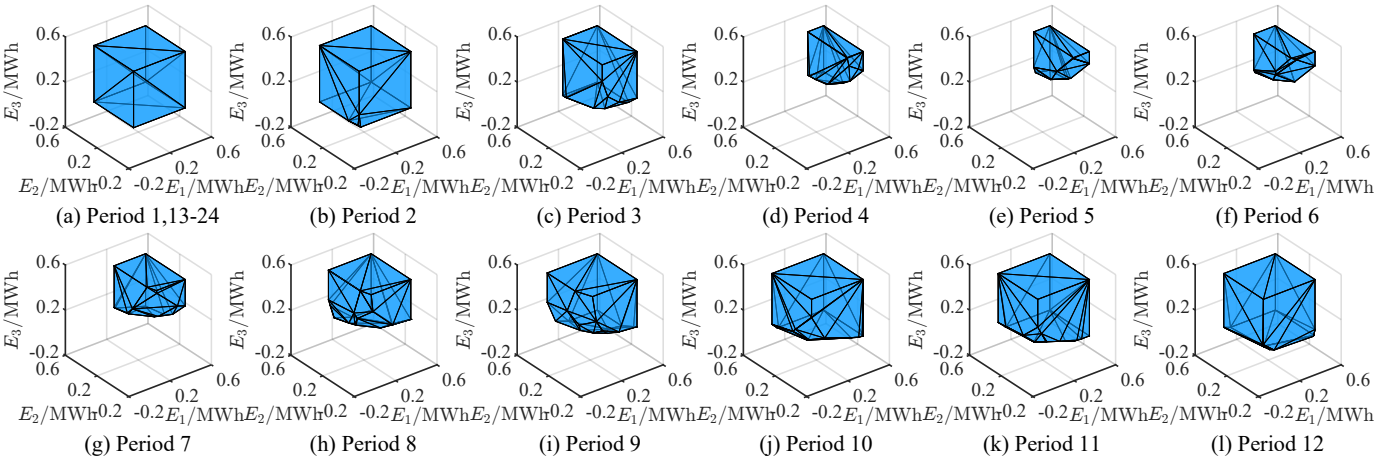

Fig. 5. Stagewise robust feasible sets of thermal storage level.

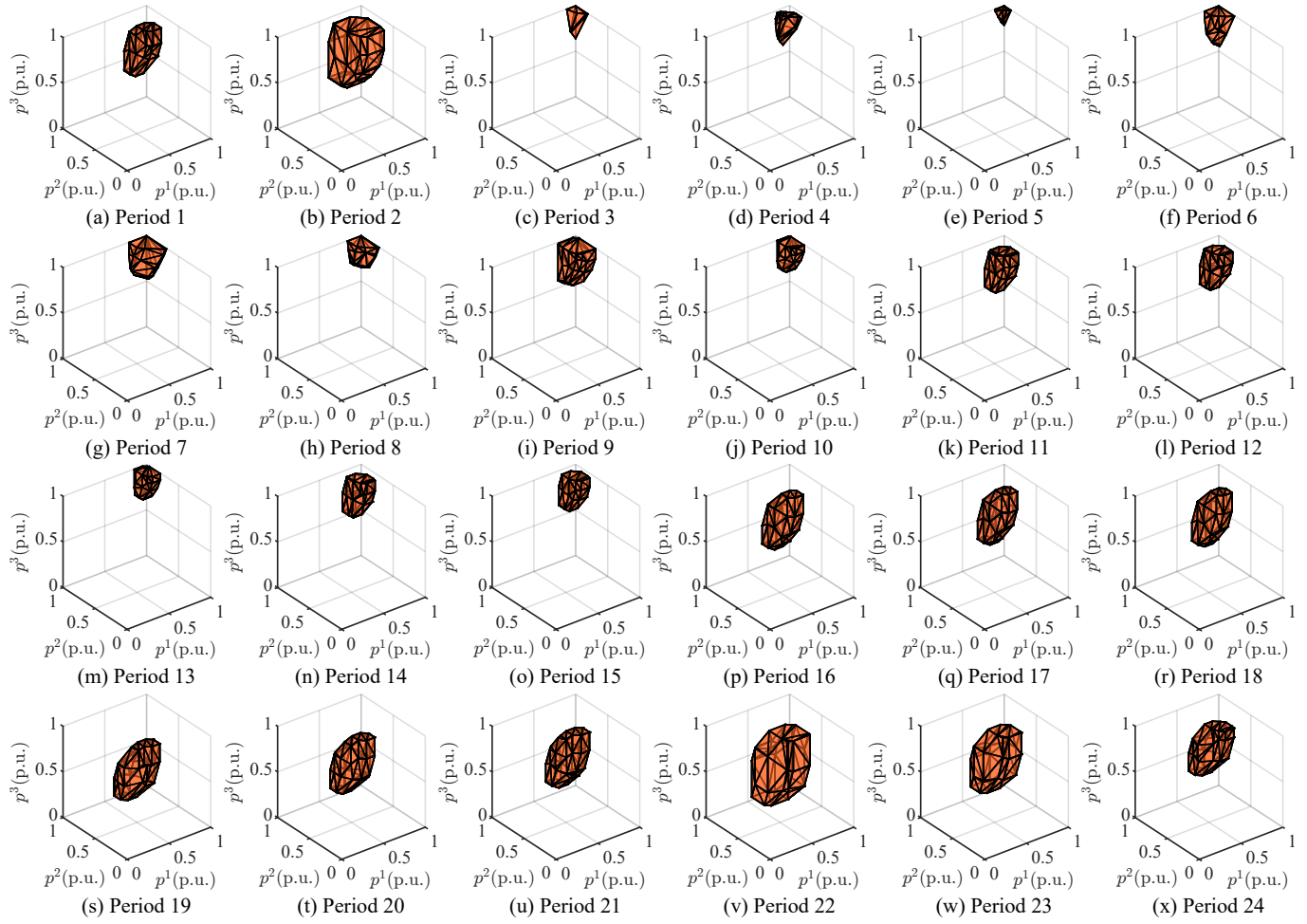

Fig. 6. Flexible loadability sets of electric heaters.

is nearly lossless, shifting the heat demand does not alter the total energy consumption in the heating system, the cost of heating system barely changes. In most periods, the power purchase under π_M is larger than that under π_{OL} and the hindsight optimum. This result emphasizes the importance of cross-system coordination.

In the greedy policy π_G, although system operation is coordinated, the dispatch strategy is myopic because its future impact is overlooked. Specifically, to save cost in the current period, π_G prioritizes the use of TES, which causes heat supply inadequacy when the stored energy is used up and renewable power is scarce at the same time. In such circumstances, delivering power from the substation to heaters is the only option, which could be infeasible due to line flow and bus

TABLE II
COMPARISON OF DIFFERENT POLICIES IN THE SMALL TESTING SYSTEM

Policy	Infeasible days	Cost (10^5\$)	Optimality gap	Renewable energy curtailment
f^*	0	4.87	baseline	10.81%
π_{OL}	0	4.98	2.26%	11.05%
π_G	68	5.09	4.52%	10.88%
π_M	0	5.39	10.68%	13.29%

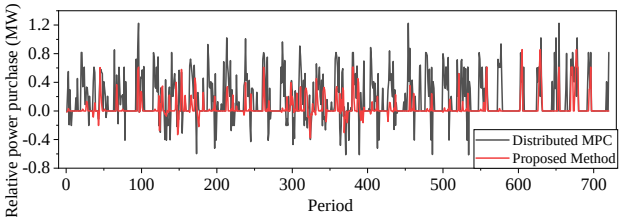

Fig. 7. Relative power purchase under different policies.

voltage limits, triggering heat load shedding. During the four months, load shedding occurs in 68 days with a total amount of 64.78MWh. Assuming the load shedding cost is 341\$/MWh, the total cost under the greedy policy π_G is 5.09×10^5\$, which is 4.52% higher than f^*. This result highlights the importance of strategic use of energy storage when the system is facing significant uncertainty.

Interestingly, from Table II we have noticed that exact forecast is not indispensable because the policy π_{OL} which involves interval forecasts can achieve fairly good performances, and furthermore, the results of π_G and π_M indicate that implementing coordination without foresight can be better than exploiting forecasts but neglecting coordination.

4) Performance in Typical Days: To show the performance of the proposed method in typical days with different renewable and demand variation patterns, we select four typical days based on the total renewable generation (high: $>$ 100MWh; low: $<$ 87MWh) and total power and heat demand (high: $>$ 137MWh; low: $<$ 93MWh).

Day-1: high renewable generation and high demand.
Day-2: high renewable generation and low demand.
Day-3: low renewable generation and high demand.
Day-4: low renewable generation and low demand.

Results are given in Table III. Among four typical days, π_{OL} outperforms π_M in terms of the cost and renewable energy curtailment rate due to the exploitation of flexibility from the heating system. The greedy policy π_G is fairly good except in Day-3, because whenever no heat load is shed, using TES with high priority is naturally a good strategy, then there is plenty of capacity to store renewable energy in case of need. If heat load shedding occurs, π_G may face penalty, as in Day-3, but greedy policy cannot identify potential load shedding due to the lack of forecasts. Nonetheless, over a long period of 4 months, the cumulative cost under π_G is even slightly lower than that of π_M, as in Table II. This might be surprising because π_G uses no forecast information while π_M knows the exact information of uncertainty. The reason is that by our definition, coordination takes place in π_G but not in π_M. Hence, exploiting the synergetic potential of heat-power integration appears to be more important than pursuing more accurate forecasts in multi-energy systems, at least in the particular scenario considered in this paper.

TABLE III
COMPARISON RESULTS IN FOUR TYPICAL DAYS

Day	Policy	Daily cost	Optimality gap	Renewable energy curtailment	Heat load shedding(MWh)
1	f^*	\$1933	baseline	9.83%	0
	π_{OL}	\$1973	2.07%	10.30%	0
	π_G	\$1940	0.36%	10.81%	0
	π_M	\$2285	18.21%	12.23%	0
2	f^*	\$601	baseline	29.68%	0
	π_{OL}	\$716	19.13%	29.70%	0
	π_G	\$601	0.00%	29.89%	0
	π_M	\$1011	68.22%	30.91%	0
3	f^*	\$5916	baseline	1.86%	0
	π_{OL}	\$5997	1.37%	1.86%	0
	π_G	\$6131	3.63%	1.86%	1.32
	π_M	\$6299	6.47%	3.16%	0
4	f^*	\$3853	baseline	7.98%	0
	π_{OL}	\$3859	0.16%	8.36%	0
	π_G	\$3853	0.00%	8.27%	0
	π_M	\$4190	8.75%	11.04%	0

B. Results for the Large System

This system is used to validate the computational efficiency. At the electric side, there are 5 wind turbines and 3 solar plants in the modified 123-bus distribution network. The 45-node district heating network includes 4 electric boilers, 2 heat pumps and 6 thermal storage units, as shown in Fig. 8. In real distribution systems, there could be more behind-the-meter resources such as distributed photovoltaic panels, which can be combined into nodal power demand. Because the operation of distribution system is adaptive to the real-time demands and involves no forecasts, behind-the-meter resources do not affect the implementation of the proposed method.

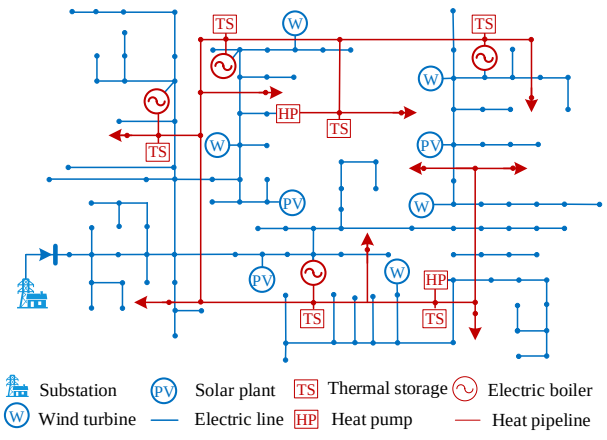

Fig. 8. Topology of the large testing system.

1) Computational Performance: The calculation times of $\mathcal{X}_t$ and $\mathcal{B}_t$ in the individual period during four months are shown in Figs. 9-10. In the day-ahead stage, Algorithm 1 takes 504 seconds on average to calculate sets $\mathcal{X}_{1:24}$ in a day. In a few periods with high heat demands, the computation is much slower. For example, at period 10 on January 13th, it takes 508 seconds to calculate $\mathcal{X}_{10}$, so the day-ahead stage consumes 18 minutes in that day. Nevertheless, there are only 4 days in which the total computation times of the day-ahead problems exceed 15 minutes, among which the longest is 19 minutes. All these days appear in January due to the high demand of heat. The time is less than 10 minutes in 90% of the days during 4 months, as shown in the last block of Fig. 9. Such a performance is satisfactory because sets $\mathcal{X}_{1:24}$ are prepared day-ahead and time is not a tight constraint.

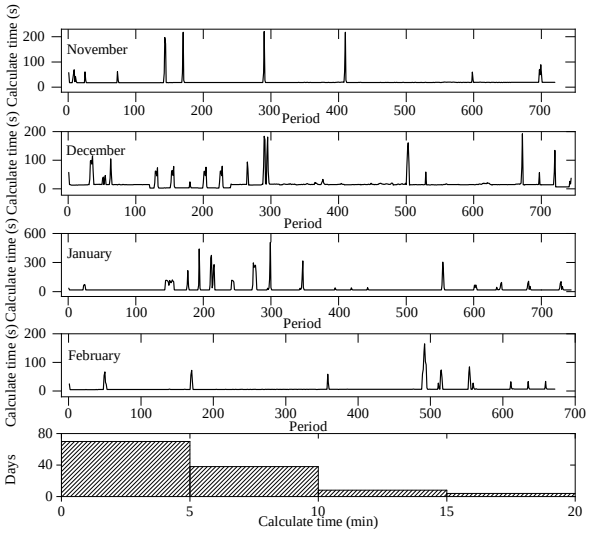

Fig. 9. Time consumption for calculating stagewise robust feasible set.

In the real-time stage, once $Q_{[d]t}$ is received at the beginning of period t, the flexible loadability set $\mathcal{B}_t$ is procured from Algorithm 1. The average (maximum) computation time of set $\mathcal{B}_t$ is 11 (54) seconds. This is still acceptable since the time is less than one minute even in the worst case, and for 90% of the 2880 periods, the time is less than 20 seconds.

2) Overall Performance Comparison: The proposed policy is compared with π_G and π_M over a period of 4 months in this large system. The results are shown in Table IV. The hindsight problem over four months results in a minimum cost of 1.085 million dollars. The hierarchical MPC policy π_M, using exact forecasts, incurs a cost of 1.223 million dollars, which is 12.7% higher due to the lack of sufficient coordination between two networks. The proposed method π_{OL} achieves a cost of 1.124 million dollars, only 3.6% higher than the hindsight optimum. For the greedy policy π_G, the operation cost is 1.144 million dollars, slightly worse than π_{OL}, because the myopic decision fails to charge TES before the peak heat demand arrives, the limited capacity of heaters triggers load shedding in the heating system.

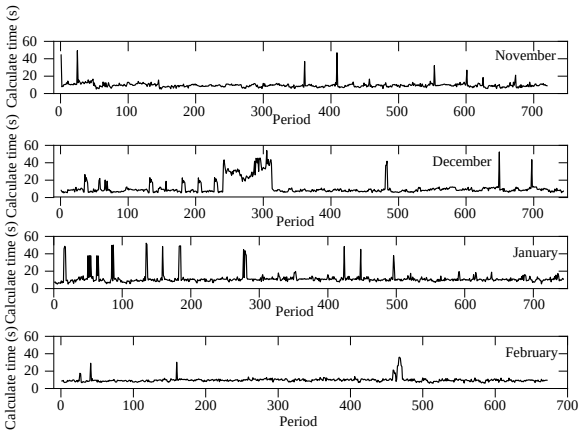

Fig. 10. Time consumption for calculating flexible loadability set.

TABLE IV
COMPARISON OF DIFFERENT POLICIES IN THE LARGE TESTING SYSTEM

Policy	Infeasible days	Cost (10^6\$)	Optimality gap	Renewable energy curtailment
f^*	0	1.085	baseline	4.0%
π_{OL}	0	1.124	3.6%	4.6%
π_G	32	1.144	5.4%	4.1%
π_M	0	1.223	12.7%	6.5%

V. CONCLUSION

This paper proposes an interactive operation method for interdependent distribution system and district heating system based on a polyhedral characterization of the heat system flexibility. It is advantageous in three aspects: first, it adopts a decentralized framework that requires least information exchange between two systems; unlike existing distributed optimization techniques which often require many iterations and fine parameter tuning, the proposed method is parameter-free and has no convergence issue. Second, it does not rely on high-quality forecasts and is adaptive to the fluctuations of renewable power and demands. Third, the distribution system is described by the nonlinear power flow model which is more accurate than linearized power flow models used in the existing works. Simulation results show that

(1) The heating system can provide considerable flexibility by submitting adjustable demands of electric heaters, contributing to a better use of renewable energy. The set calculation takes less than a minute on average, which is sufficiently fast for practical usage. Without battery storage, renewable power forecast is unnecessary, and the system-level coordination is important in cost reduction.

(2) In any circumstance, the proposed method is no inferior compared to its competitors. On average, it reduces the cost by 1.8% (8.8%) compared to the centralized greedy policy (hierarchical MPC policy), and achieves an average optimality gap of 3.6% compared to the hindsight optimum.

The proposed framework is quite general and can be easily extended to other applications, such as operating a microgrid and multiple virtual power plants. The ongoing work is to develop robust data-driven methods that better exploits historical

data, forecast information and operation experiences, aiming to circumvent the subjectivity and conservativeness in selecting the demand uncertainty set, while achieving a proper tradeoff between cost and potential risk.

REFERENCES

[1] S. Impram, S. V. Nese, and B. Oral, "Challenges of renewable energy penetration on power system flexibility: A survey," *Energy Strategy Rev.*, vol. 31, p. 100539, Sep. 2020.

[2] M. Stecca, L. R. Elizondo, T. B. Soeiro, P. Bauer, and P. Palensky, "A comprehensive review of the integration of battery energy storage systems into distribution networks," *IEEE Open J. Ind. Electron. Soc.*, vol. 1, pp. 46–65, Mar. 2020.

[3] I. Dincer and M. A. Rosen, *Thermal Energy Storage: Systems and Applications*. UK: John Wiley & Sons, 2021.

[4] B. Liu, J. Li, S. Zhang, M. Gao, H. Ma, G. Li, and C. Gu, "Economic dispatch of combined heat and power energy systems using electric boiler to accommodate wind power," *IEEE Access*, vol. 8, pp. 41 288–41 297, Jan. 2020.

[5] A. S. Gaur, D. Z. Fitiwi, and J. Curtis, "Heat pumps and our low-carbon future: A comprehensive review," *Energy Res. Soc. Sci.*, vol. 71, p. 101764, Jan. 2021.

[6] A. Benonysson, "Dynamic modelling and operational optimization of district heating systems," Ph.D. dissertation, Technical University of Denmark, 1991.

[7] X. Liu, J. Wu, N. Jenkins, and A. Bagdanavicius, "Combined analysis of electricity and heat networks," *Appl. Energy*, vol. 162, no. 15, pp. 1238–1250, Jan. 2016.

[8] Z. Li, W. Wu, M. Shahidehpour, J. Wang, and B. Zhang, "Combined heat and power dispatch considering pipeline energy storage of district heating network," *IEEE Trans. Sustain. Energy*, vol. 7, no. 1, pp. 12–22, Jan. 2016.

[9] H. Zhou, Z. Li, J. H. Zheng, Q. H. Wu, and H. Zhang, "Robust scheduling of integrated electricity and heating system hedging heating network uncertainties," *IEEE Trans. Smart Grid*, vol. 11, no. 2, pp. 1543–1555, Mar. 2020.

[10] L. Moretti, E. Martelli, and G. Manzolini, "An efficient robust optimization model for the unit commitment and dispatch of multi-energy systems and microgrids," *Appl. Energy*, vol. 261, no. 1, p. 113859, Mar. 2020.

[11] Y. Zhou, M. Shahidehpour, Z. Wei, G. Sun, and S. Chen, "Multistage robust look-ahead unit commitment with probabilistic forecasting in multi-carrier energy systems," *IEEE Trans. Sustain. Energy*, vol. 12, no. 1, pp. 70–82, Jan. 2021.

[12] Y. Zhou, Q. Zhai, M. Zhou, and X. Li, "Generation scheduling of self-generation power plant in enterprise microgrid with wind power and gateway power bound limits," *IEEE Trans. Sustain. Energy*, vol. 11, no. 2, pp. 758–770, Apr. 2020.

[13] S. Feng, W. Wei, and Y. Chen, "Day-ahead scheduling and online dispatch of energy hubs: A flexibility envelope approach," *IEEE Trans. Smart Grid*, vol. 15, no. 3, pp. 2723–2737, May 2024.

[14] H. Xiong, Z. Chen, X. Zhang, C. Wang, Y. Shi, and C. Guo, "Robust scheduling with temporal decomposition of integrated electrical-heating system based on dynamic programming formulation," *IEEE Trans. Ind. Appl.*, vol. 59, no. 4, pp. 5087–5100, July-Aug. 2023.

[15] Y. Cao, W. Wei, L. Wu, S. Mei, M. Shahidehpour, and Z. Li, "Decentralized operation of interdependent power distribution network and district heating network: A market-driven approach," *IEEE Trans. Smart Grid*, vol. 10, no. 5, pp. 5374–5385, Sep. 2019.

[16] Y. Chen, W. Wei, F. Liu, E. E. Sauma, and S. Mei, "Energy trading and market equilibrium in integrated heat-power distribution systems," *IEEE Trans. Smart Grid*, vol. 10, no. 4, pp. 4080–4094, Jul. 2019.

[17] C. Lin, W. Wu, B. Zhang, and Y. Sun, "Decentralized solution for combined heat and power dispatch through Benders decomposition," *IEEE Trans. Sustain. Energy*, vol. 8, no. 4, pp. 1361–1372, Oct. 2017.

[18] J. Li, J. Fang, Q. Zeng, and Z. Chen, "Optimal operation of the integrated electrical and heating systems to accommodate the intermittent renewable sources," *Appl. Energy*, vol. 167, no. 1, pp. 244–254, Apr. 2016.

[19] B. Chen, W. Wu, and H. Sun, "Coordinated heat and power dispatch considering mutual benefit and mutual trust: A multi-party perspective," *IEEE Trans. Sustain. Energy*, vol. 13, no. 1, pp. 251–264, Jan. 2022.

[20] W. Zheng, J. Zhu, and Q. Luo, "Distributed dispatch of integrated electricity-heat systems with variable mass flow," *IEEE Trans. Smart Grid*, vol. 14, no. 3, pp. 1907–1919, May 2023.

[21] C. Yang and Z. Li, "Distributed conditional-distributionally robust coordination for an electrical power and flexibility-enhanced district heating system," *Appl. Energy*, vol. 347, no. 1, p. 121491, Oct. 2023.

[22] J. Tan, Q. Wu, W. Wei, F. Liu, C. Li, and B. Zhou, "Decentralized robust energy and reserve co-optimization for multiple integrated electricity and heating systems," *Energy*, vol. 205, no. 15, p. 118040, Aug. 2020.

[23] L. Zhao, W. Zhang, H. Hao, and K. Kalsi, "A geometric approach to aggregate flexibility modeling of thermostatically controlled loads," *IEEE Trans. Power Syst.*, vol. 32, no. 6, pp. 4721–4731, Nov. 2017.

[24] B. Zheng, W. Wei, Y. Xu, and Y. Chen, "Capacity aggregation and online control of clustered energy storage units," *IEEE Trans. Sustain. Energy*, vol. 15, no. 3, pp. 1546–1561, Jul. 2024.

[25] X. Xu, Q. Lyu, M. Qadrdan, and J. Wu, "Quantification of flexibility of a district heating system for the power grid," *IEEE Trans. Sustain. Energy*, vol. 11, no. 4, pp. 2617–2630, Oct. 2020.

[26] S. Lu, W. Gu, K. Meng, S. Yao, B. Liu, and Z. Y. Dong, "Thermal inertial aggregation model for integrated energy systems," *IEEE Trans. Power Syst.*, vol. 35, no. 3, pp. 2374–2387, May 2020.

[27] W. Zheng, W. Wu, Z. Li, H. Sun, and Y. Hou, "A non-iterative decoupled solution for robust integrated electricity-heat scheduling based on network reduction," *IEEE Trans. Sustain. Energy*, vol. 12, no. 2, pp. 1473–1488, Apr. 2021.

[28] M. Farivar and S. H. Low, "Branch flow model: Relaxations and convexification-Part I," *IEEE Trans. Power Syst.*, vol. 28, no. 3, p. 2554–2564, Aug. 2013.

[29] L. Gan, N. Li, U. Topcu, and S. H. Low, "Exact convex relaxation of optimal power flow in radial networks," *IEEE Trans. Autom. Control.*, vol. 60, no. 1, pp. 72–87, Jan. 2015.

[30] *Electric Heating Boilers Technical Conditions*, The People's Republic of China Std. NB/T 10 936-2022, 2022.

[31] P. Carroll, M. Chesser, and P. Lyons, "Air source heat pumps field studies: a systematic literature review," *Renew. Sustain. Energy Rev.*, vol. 134, p. 110275, Dec. 2020.

[32] J. Luo, J. Rohn, W. Xiang, D. Bertermann, and P. Blum, "A review of ground investigations for ground source heat pump (GSHP) systems," *Energy Build.*, vol. 117, no. 1, pp. 160–175, Apr. 2016.

[33] W. Wei, F. Liu, and S. Mei, "Real-time dispatchability of bulk power systems with volatile renewable generations," *IEEE Trans. Sustain. Energy*, vol. 6, no. 3, pp. 738–747, Jul. 2015.

[34] H. Konno, "A cutting plane algorithm for solving bilinear programs," *Math. Program.*, vol. 11, pp. 14–27, Dec. 1976.

[35] P. C. Chen, P. Hansen, and B. Jaumard, "On-line and off-line vertex enumeration by adjacency lists," *Oper. Res. Lett.*, vol. 10, no. 7, pp. 403–409, Oct. 1991.

[36] D. Bertsimas and J. N. Tsitsiklis, *Introduction to Linear Optimization*. Belmont, MA: Athena Scientific, 1997.

[37] Z. Li, Q. Guo, H. Sun, and J. Wang, "Extended sufficient conditions for exact relaxation of the complementarity constraints in storage-concerned economic dispatch," *CSEE J. Power Energy Syst.*, vol. 4, no. 4, pp. 504–512, Dec. 2018.

[38] M. E. Baran and F. F. Wu, "Network reconfiguration in distribution systems for loss reduction and load balancing," *IEEE Trans. on Power Delivery*, vol. 4, no. 2, pp. 1401–1407, Apr. 1989.

[39] Z. Shen, W. Wei, T. Ding, Z. Li, and S. Mei, "Admissible region of renewable generation ensuring power flow solvability in distribution networks," *IEEE Syst. J.*, vol. 16, no. 3, pp. 3982–3992, Sep. 2022.

[40] W. Chen, "the coupled systems data," 2024. [Online]. Available: https://github.com/weitao-chen/the_coupled_systems_data

APPENDIX

Detailed models of the three competitors are listed below.

Hindsight optimum: Assume the coupled systems is centrally operated. At the end of a day, the heat demand data is known exactly. So the ideal minimum cost f^* can be obtained by solving a deterministic optimization problem

$$\begin{aligned} f^* = \min \quad & \sum_{t\in T}\sum_{j\in\delta(0)} \rho_t P_{0j,t} \\ \text{s.t.} \quad & \text{heating system model (1)} \\ & \text{branch flow model (2)} \\ & \text{heater model (3)} \end{aligned} \tag{22}$$

The hindsight optimum f^* cannot be achieved in practice. It is a baseline that quantifies the optimality gap of a given policy π. Let $f(\pi)$ is the actual cost under policy π, the optimality gap is $v^* = (f(\pi) - f^*)/f^*$. Clearly, for any policy that does not use exact prediction, we have $v^* > 0$.

Centralized greedy method: Still in a centralized framework, the greedy policy π_G makes a decision based on the current observation of the uncertainty, yielding

$$\begin{aligned} \min \quad & \rho_t \sum\nolimits_{j\in\delta(0)} P_{0j} \\ \text{s.t.} \quad & \text{heating system model (1)} \\ & \text{branch flow model (2)} \\ & \text{heater model (3)} \end{aligned} \tag{23}$$

Unlike (22) which optimizes actions across the day, problem (23) pertains to a single period t. Parameters ρ_t, $Q_{[d]t}$ and x_{t-1} are revealed at the beginning of this period, and no predictive information is needed. Since the future impact of the current action is neglected, π_G is myopic and thus suboptimal, especially when the heating system is heavily loaded.

Hierarchical MPC: Assume the distribution system and the heating system make decisions individually. In particular, the heating system predicts heat demands in the next 24 hours and solves a minimum loss problem, then submits the power demand of heaters in the current period to the distribution system. The dispatch actions can be retrieved from optimal power flow. The flowchart of the hierarchical model predictive control (MPC) policy π_M is provided in Algorithm 3.

Algorithm 3 : Hierarchical MPC

1: **District heating system**: observe $(x_{t-1}, Q_{[d]t})$, predict heat demands in the next n periods. Solve the following lookahead dispatch problem

$$\begin{aligned} \min_{x_\tau, y^{\text{in}}_\tau, y_{[h]\tau}} \quad & \sum_{\tau=t}^{t+n} \sum_{b} \left(T^{\text{in}}_{b\tau} - T^{\text{out}}_{b\tau}\right) \\ \text{s.t.} \quad & (y_{[h]\tau}, y^{\text{in}}_\tau, x_\tau) \in \mathcal{F}_\tau(x_{\tau-1}, Q_{[d]\tau}), \forall \tau \\ & \text{heater model (3)} \end{aligned} \tag{24}$$

and submit heater power demands $p_t^{[h]}$ to the distribution system.

2: **Distribution system**: receive heater power demands $p_t^{[h]}$, observe the renewable power and nodal loads in the current period, solve the following optimal power flow problem

$$\begin{aligned} \min \quad & \rho_t \sum\nolimits_{j\in\delta(0)} P_{0j} \\ \text{s.t.} \quad & \text{branch flow model (2)} \end{aligned} \tag{25}$$

Then proceed to the next period.

In our tests, we assume the prediction of heat load $Q_{[d]t}$ is exact, which is favored by MPC. In practice, the performance of MPC can be inferior due to forecast errors. In this method, the heating system submits fixed demands of electric heaters which are restrictive lack flexibility. In contrast, in the proposed method, the heating system submits a set $\mathcal{B}_t$ of admissible demands which allows a more flexible dispatch and encourages coordination between the distribution network and the district heating network.

Weitao Chen (Graduate Student Member, IEEE) received the B.S. degree in electrical engineering from China Agricultural University, Beijing, China, in 2018, she is currently working toward pursuing the Ph.D. degree with Beijing Jiaotong University, Beijing, China. Her research interests include operation of interdependent power system and heating system.

Xiaojun Wang (Senior Member, IEEE) received the B.S., M.S., and Ph.D. degrees in electrical engineering from North China Electric Power University, Beijing, China, in 2001, 2004, and 2008, respectively. He is currently a Professor with Beijing Jiaotong University, Beijing.

His research interests include power system analysis and control, modeling and analysis of multi-energy supplement system, fault diagnosis and location of distribution network, and power quality.

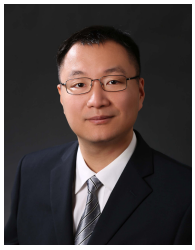

Wei Wei (Senior Member, IEEE) received the B.Sc. and Ph.D. degrees in electrical engineering from Tsinghua University, Beijing, China, in 2008 and 2013, respectively.

From 2013 to 2015, he was a Postdoctoral Research Associate with Tsinghua University. He was a Visiting Scholar with Cornell University, Ithaca, NY, USA, in 2014, and a Visiting Scholar with Harvard University, Cambridge, MA, USA, in 2015. He is currently an Associate Professor with Tsinghua University. His research interests include applied optimization and energy system economics.

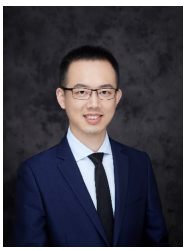

Yin Xu (Senior Member, IEEE) received the B.E. and Ph.D. degrees in electrical engineering from Tsinghua University, Beijing, China, in 2008 and 2013, respectively. During 2013-2016, he was an Assistant Research Professor with the School of Electrical Engineering and Computer Science, Washington State University, Pullman, WA,USA. He is currently a Professor with Beijing Jiaotong University, Beijing. His research interests include power system resilience and power system dynamics.

Dr. Xu is currently serving as Chair of the Energy Internet Resilience Working Group under the IEEE PES Energy Internet Coordinating Committee and Secretary of the Distribution Test Feeder Working Group under the IEEE PES Distribution System Analysis Subcommittee. He is an Editorial Broad member of IEEE Transactions on Power Systems, IEEE Power Engineering Letters, IET Smart Grid, Energy Conversion and Economics, and Energy Internet.

Jianzhong Wu (Fellow, IEEE) received his B.Sc., M.Sc., and Ph.D. degrees in electrical engineering from Tianjin University, China, in 1999, 2002 and 2004, respectively. From 2004 to 2006, he was at Tianjin University as a postdoctoral researcher and then an Associate Professor. From 2006 to 2008, he was a Research Fellow at the University of Manchester, UK. He joined Cardiff University in 2008 and is currently a Professor of Multi-Vector Energy Systems and Head of the School of Engineering. His research interests include integrated multi-energy infrastructure and smart grids. He is Co-Editor-in-Chief of Applied Energy, Co-Director of the UK Energy Research Centre and the EPSRC Supergen Energy Networks Impact Hub, and a Fellow of the Energy Institute and the Learned Society of Wales.